

Original article

Development of Local Conversion Models to Estimate the Electrical Conductivity of Saturated Soil Paste Extracts from Water Dilution Extracts (1:1, 1:2, 1:5) in the Haflez and Kambut Depressions, Eastern Tobruk, Libya

Mohammed Abas 

Department of Natural Resources, Faculty of Natural Resources and Environmental Sciences, University of Tobruk, Tobruk, Libya

Email: Mohmed.boabss@tu.edu.ly

Abstract

This study aimed to develop local conversion models between E_{Ce} and extract dilution ratios (1:1, 1:2, 1:5) in three semi-arid depressions in eastern Libya. A total of 45 surface soil samples (0–20 cm) were collected from the Hafilz (HZ), Southern Kambout (K1), and Northern Kambout (K2) depressions, following a stratified-spatial sampling design. Laboratory analyses were conducted using standard methods, and linear and quadratic regression models were developed, with performance evaluated using R², RMSE, and five-fold cross-validation. The results showed significant variation in salinity between the depressions ($p < 0.001$), with K2 recording the highest average (9.40 dS m⁻¹). Quadratic models outperformed linear ones, especially at high salinity levels (R² ≈ 0.995 for 1:1), with high stability in cross-validation. ANCOVA analysis revealed differences in conversion coefficients between the depressions ($p < 0.05$), emphasizing the need for local calibration. The study recommends using the 1:1 extract ratio as the primary operational model, with quadratic models applied in high-salinity environments.

Keywords. Soil Salinity, E_{Ce}, Dilution Extracts, Quadratic Regression, Tobruk.

Introduction

Soil salinity is one of the major environmental constraints that affect agricultural production in arid and semi-arid environments, as the accumulation of dissolved salts in the soil contributes to the decline of its physical and chemical properties. The Electrical Conductivity of Saturated Paste (E_{Ce}) is considered the standard indicator used to evaluate soil salinity because it reflects the concentration of ions in the soil solution under near-natural conditions [1]. Therefore, E_{Ce} is the most reliable indicator for assessing crop salt tolerance and making irrigation and agricultural management decisions [2].

However, the preparation of the saturated paste and extraction of the solution is a labor-intensive process that consumes a lot of time and requires large quantities of soil and distilled water, making it impractical for large-scale field studies or in laboratories with limited resources [3]. For this reason, water dilution extracts such as 1:1, 1:2, and 1:5 are used as practical alternatives due to their simplicity and ease of application. However, the relationship between dilution extracts and E_{Ce} is influenced by several factors, such as soil texture, prevailing salt types, and gypsum content, which necessitates the development of local empirical models [4].

Many studies have shown a linear relationship between E_{Ce} and the EC measured in different water extracts. However, using general or international conversion equations may lead to significant estimation errors, especially in soils with very high salinity, where linear relationships lose their accuracy [5]. Additionally, studies addressing this relationship in geographically closed regions with specific topographical features, such as semi-arid depressions, are very few. These closed depressions are subject to intense spatial variation and non-linear salt accumulation, making it unreliable to transfer equations from other regions. Furthermore, comparative evaluation of linear and non-linear models within different dilution ratios in the same environmental context remains limited. There is also a need to test the slope/gradient differences between depressions (i.e., is one equation enough, or is a model required for each depression?).

This variation in results reflects the need for local calibration of the equations used, as environmental factors and soil characteristics can lead to significant differences in the relationship between dilution extracts and E_{Ce}. While most studies rely on simple linear regression, the relationship between E_{Ce} and dilution extracts may be non-linear in some cases, especially when salinity levels span a wide range. Therefore, non-linear conversion models such as quadratic or exponential models have been proposed to improve prediction accuracy [6]. However, the evaluation of the performance of non-linear models compared to linear models is context-dependent and should be selected based on predictive stability analysis and simplicity.

Accurate model evaluation not only depends on calibration but also includes testing their ability to generalize to avoid overfitting, especially when dealing with moderately sized samples. Thus, cross-validation has become a standard method for evaluating generalization in environmental regression modeling [7]. Furthermore, indicators such as the coefficient of determination (R²) and the root mean square error (RMSE) provide complementary information about predictive error and deviation size in the original measurement unit [8]. Therefore, this paper aims to study the correlation relationships between E_{Ce} and extracts (1:1,

1:2, 1:5) in the soils of Haflez and Kambout depressions, derive mathematical equations (linear or non-linear) characterized by accuracy and statistical efficiency, and evaluate model stability using cross-validation to identify the most suitable model for practical application in semi-arid soil environments, to facilitate salinity estimation in local laboratories.

Study Area

The three study areas are located to the east and southeast of the city of Tobruk, Libya (Figure 1). The Kambout area is approximately 60 km east of Tobruk, while the Haflez area is about 10 km south of Kambout.

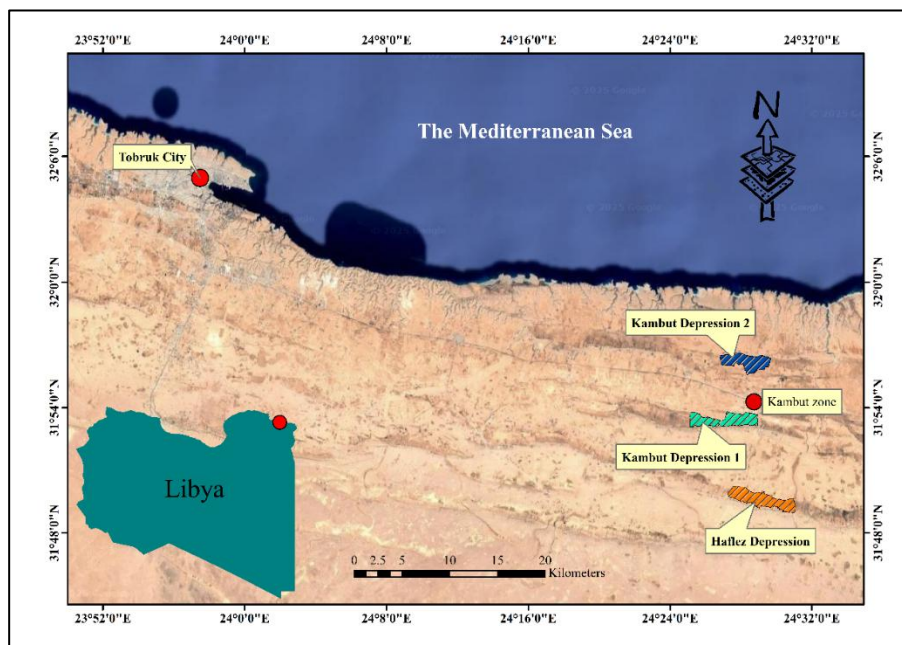


Figure 1. Geographic location of the study area

The first depression, Haflez Depression (HZ), is located approximately 17 km from the Mediterranean coast. The second depression, Southern Kambout Depression (K1), is about 11 km from the coast. The third depression, Northern Kambout Depression (K2), is approximately 5 km from the coast.

Geographically, the maps derived from the Digital Elevation Model (DEM) (Figure 2) illustrate the topographic and slope variation within the Haflez and Kambout depressions. The elevation in Haflez ranges between – 129 and 142 meters, with a gradual increase toward the southern edge. The contour lines indicate slightly undulating terrain, interspersed with mild depressions in the central part. In contrast, the Kambout depression shows lower elevations, with Kambout 1 ranging between 92 and 117 meters, and Kambout 2 between 75 and 83 meters.

Slope maps reveal that very low slopes (0–2%) dominate all study areas within Haflez, Kambout 1, and Kambout 2 depressions, reflecting the gently sloping surface typical of semi-flat depositional environments. In Haflez, the 0–1% slope category covers an area of approximately 281 km², followed by the 1–2% slope category with an area of 229 km², meaning over 80% of the depression's area has a gentle slope, while slopes steeper than 3% cover a limited area of less than 5%. Similarly, Kambout 1 shows a similar pattern, with 0–2% slopes covering around 395 km² of the total area, and a gradual decrease in higher slope categories (2–3% = 77.7 km² and 4–6% = 5.3 km²). In Kambout 2, the 0–1% and 1–2% categories are almost equal in area (183 and 197 km², respectively), while slopes steeper than 3% constitute a small percentage of just under 6%. These results collectively indicate that all three depressions feature relatively flat surfaces with very gentle slopes, making them favorable environments for fine sediment accumulation and the formation of saline soils, while also limiting the efficiency of surface drainage, consistent with their geomorphological nature as closed depressions with internal drainage.

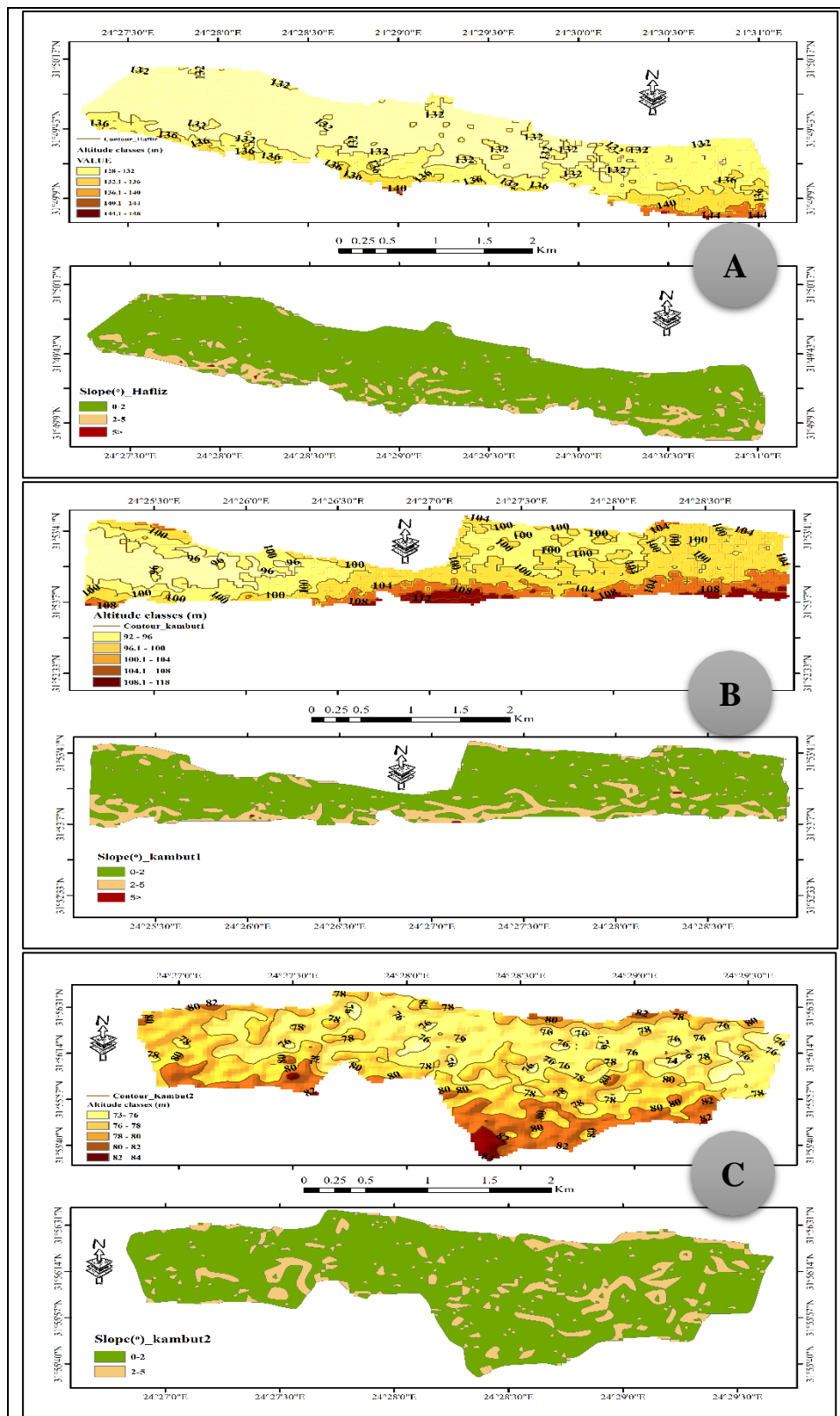


Figure 2. Elevation and slope maps for Haflez (A) and Kambout1 (B) & 2 (C) depressions in eastern Libya.

The upper panels show elevation categories derived from the Digital Elevation Model, while the lower panels show slope categories in percentage.

Climatically, there is no published study specifically addressing the extended climatic changes in the Kambout area, and there is no nearby meteorological station except for the one in Tobruk city. Therefore, we rely on the climate data for Tobruk, which experiences a semi-arid Mediterranean climate characterized by mild, rainy winters and hot, dry summers. The region is influenced by continental desert air masses from the south and marine tropical air masses from the Mediterranean during winter. Annual temperatures range from 13 to 31°C, with relative humidity reaching about 91% in August. The annual rainfall varies between

80 and 180 mm, concentrated in winter (about 64%), while it is almost nonexistent in summer. Rainfall shows clear annual fluctuations and a weak to moderate positive correlation with the North Atlantic Oscillation (NAO), and the prevailing northwestern winds contribute to increased evaporation, creating semi-arid conditions in the region [9].

Regarding water resources, both Haflez and Kambout suffer from surface water scarcity, relying heavily on limited amounts of water collected from rainfall, which the local population gathers by digging wells (water traps). Groundwater levels range from 135 to 190 meters and have high salinity (3000–6000 ppm), making them unsuitable for irrigation under normal conditions. The soil is also poor and highly alkaline [10]. The local population depends on traditional rain-fed farming for crops such as barley and some vegetables, utilizing the residual moisture in the soil.

Methods

Sampling Design

The study adopted a Stratified Spatial Sampling Design due to the heterogeneous nature of salinity distribution within the semi-arid depressions. Geomorphological and hydrological studies indicate that salt accumulation in depressions is directly influenced by topographic gradients, surface flow pathways, and final accumulation sites [11].

Based on this, the depression was divided into three sectors (western, central, and eastern) to represent the topographic gradient, and samples were distributed longitudinally from the edge of the depression to the center of accumulation and its opposite end. This ensures the representation of salt reception areas and final accumulation, while minimizing spatial bias, which aligns with the recommendations from studies on spatial variation and topographic control in semi-arid environments [12-15].

A total of 45 composite samples were collected in October 2026 from a depth of 0–20 cm, with 5 samples taken from each sector, amounting to 15 samples per depression. Each composite sample represented nine (9) sub-samples from within a circular area of approximately 10 meters in diameter, arranged in an "X-pattern" to ensure good distribution and accurate spatial representation of the surrounding area at each point. After collecting the sub-samples, they were mixed thoroughly in a clean plastic container to obtain a homogeneous composite sample, and about 1000 grams were taken for laboratory analysis. The geographical coordinates and elevation for each location were recorded using a GPS device.

Laboratory Analyses

All laboratory analyses were conducted at the Faculty of Natural Resources and Environmental Sciences, Tobruk University, following internationally recognized standard protocols. The pH and electrical conductivity were measured using standard analytical methods, and particle size distribution was determined by the hydrometer method as outlined in [16].

The saturated paste extract (EC_e) was prepared following the reference method of Richards (1954). Distilled water was gradually added to 250 g of dry, air-dried soil until the soil reached the point of apparent saturation. The paste was left for 18 hours to achieve water equilibrium, then the leachate was extracted by filtration under vacuum using Whatman No. 42 filter paper. The electrical conductivity of the leachate was measured at 25°C using a calibrated conductivity meter.

For the dilution extracts of 1:1, 1:2, and 1:5 (soil: water, weight/volume), 100 mL of distilled water was added to 100 g, 50 g, and 20 g of soil, respectively. The samples were mechanically shaken for 30 minutes to ensure homogeneity, then left for 18 hours to reach equilibrium before filtration using the same procedure as for the saturated paste extract.

To ensure analytical precision and reproducibility, quality control procedures were applied, including daily calibration of the conductivity meter using certified, traceable standards at 25°C (the meter automatically compensates and corrects the measurements to 25°C). The accepted deviation was checked before measurement, and duplicate analyses were conducted for at least 10% of randomly selected samples. Results were accepted if the relative difference between measurements did not exceed ±5%. High-purity distilled water (EC < 0.01 dS m⁻¹) was used for all preparations to avoid ionic contamination. Glassware was cleaned and treated between samples to prevent cross-contamination.

Statistical Analysis

The analyses were performed using SPSS v26 at a significance level of ($\alpha = 0.05$). A simple linear regression model was developed using Ordinary Least Squares (OLS) to represent the relationship between the electrical conductivity of the saturated paste extract (EC_e) and one of the dilution extracts (X) as per the equation:

$$EC_e = \beta_0 + \beta_1 X$$

Given the wide range of salinity in some locations and the potential for deviation from linearity at high ionic strength levels, a second-degree quadratic regression model was tested:

$$EC_e = \beta_0 + \beta_1 X + \beta_2 X^2$$

The performance of the linear and quadratic models was compared using the coefficient of determination (R^2), adjusted R^2 , root mean square error (RMSE), and out-of-sample performance indicators via five-fold cross-validation to assess predictive ability and reduce the likelihood of overfitting [7,8].

Since the study includes three depressions with different geomorphological and salinity characteristics, Analysis of Covariance (ANCOVA) was used to test if the relationship between ECe and the dilution extracts differs between depressions. The model included testing the effect of depression (a categorical factor), the continuous variable (extract), and their interaction term, according to the general formula:

$$ECe = \beta_0 + \beta_1 X + \beta_2 D + \beta_3 (X \times D)$$

Where D represents the depression factor, and the interaction term ($X \times D$) directly tests the difference in the slope of the relationship between depression. This test is essential to determine whether a general conversion equation can be applied across all depressions or if local calibration is required for each depression, which is a key methodological question in salinity modeling studies [17].

High-influence values were examined using Cook's Distance, with the threshold of $(4/n)$ applied to identify potential influential points, and sensitivity analysis was conducted when necessary.

Differences between depressions were tested using One-way ANOVA followed by Tukey HSD post-hoc testing at the same significance level. Additionally, the performance of the models was evaluated across four salinity categories ($0-2$, $2-4$, $4-10$, and >10 dS m^{-1}) to determine the applicability range and stability of the relationship across different salinity levels.

Results and Discussion

Spatial Variation of the Salinity System in the Three Depressions

ECe values showed a clear variation between the three depressions (Table 1). The average ECe in the Northern Kambout Depression (K2) was 9.40 ± 7.16 dS m^{-1} , compared to 2.17 ± 2.25 dS m^{-1} in Haflez (HZ) and 2.06 ± 2.61 dS m^{-1} in Southern Kambout (K1). The range of values in K2 ($0.85-18.8$ dS m^{-1}) was wider compared to HZ ($0.8-9.4$) and K1 ($0.6-10.6$).

Table 1. Descriptive statistics for the three depressions

Depression	n	ECe_mean	ECe_sd	ECe_min	ECe_max	pH_mean	pH_sd
Hafilz	15	2.173333	2.249275	0.8	9.4	7.914667	0.167965
Kampot1	15	2.064667	2.608176	0.6	10.6	7.981333	0.170665
Kampot2	15	9.396667	7.163161	0.85	18.8	7.733333	0.2303

One-way ANOVA confirmed significant differences between the depressions ($F(2,42) = 12.58$, $p < 0.001$), and when Tukey HSD was used to determine the differences between the three depressions in this study, the results showed a significant difference between Kambout 2 and the other depressions (Haflez and Kambout 1), indicating a substantial difference in the intensity of the salinity system between the depressions. This is consistent with the closed nature of the depressions, where weak surface drainage limits leaching efficiency, and high evaporation leads to the re-concentration of salts in accumulation zones [1]. The wide standard deviation in K2 reflects higher internal variation, which increases the likelihood of non-linear behavior in conversion relationships. This further supports the need for local calibration rather than using a general conversion equation.

Table 2. ANOVA Test Results

	sum_sq	df	F	PR(>F)
C(Depression)	529.7329	2	12.57821	0.0000524
Residual	884.4178	42	--	--

Table 3. Tukey Test Results

group1	group2	meandiff	p-adj	lower	upper	reject
Hafilz	Kampot1	-0.1087	0.9977	-4.1796	3.9622	FALSE
Hafilz	Kampot2	7.2233	0.0003	3.1524	11.2942	TRUE
Kampot1	Kampot2	7.332	0.0002	3.2611	11.4029	TRUE

Linear Model

The linear regression model between ECe and EC(1:1) showed a high R^2 value ($R^2 = 0.934$, Adjusted $R^2 = 0.933$), with RMSE = 1.44 dS m^{-1} and CV- $R^2 = 0.89$. For EC(1:2), the R^2 was 0.910 , and the RMSE was 1.68 dS m^{-1} . In contrast, the performance of EC(1:5) was lower ($R^2 \approx 0.69$).

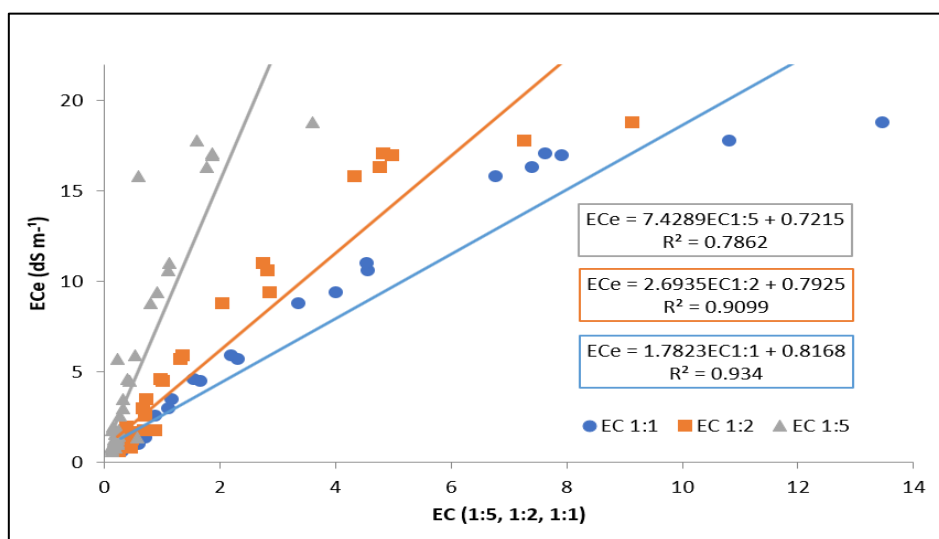


Figure 3. Linear model E_{Ce} vs. (EC 1:1, 1:2, 1:5)

These results confirm that the 1:1 and 1:2 extracts maintain high explanatory power, reflecting the concentration similarity between the extracted solution and the semi-saturated conditions. However, when analyzing the residuals, a non-linear deviation was observed at high salinity levels, especially in Kambout 2, suggesting that the linear hypothesis may not be sufficient across the full salinity range. Based on this, a quadratic model was used to improve prediction accuracy in such cases.

Quadratic Model

The CV- R^2 value is an important indicator of model stability, as it reflects the model's ability to generalize across different salinity categories. In this study, the quadratic models showed superior performance with CV- R^2 (Table 4), where the R^2 for 1:1 increased to $R^2 = 0.995$ (Adjusted $R^2 = 0.995$), and RMSE decreased to 0.41 dS m^{-1} , a relative error reduction of $\sim 71\%$ compared to the linear model (Figure 4). The CV- R^2 reached 0.992, indicating high predictive stability. For 1:2, R^2 increased to 0.990, while for 1:5, R^2 was about 0.90 after data correction. This indicates high stability in predictions across different salinity categories. This improvement in predictive performance reflects the high adaptability of the quadratic model to changing salinity data.

Table 4. Comparison of linear and quadratic models

Extract Ratio	Linear R^2	Linear RMSE	Quadratic R^2	Quadratic RMSE
1:1	0.934	1.440	0.995	0.410
1:2	0.910	1.684	0.990	0.566
1:5	0.786	2.592	0.902	1.755

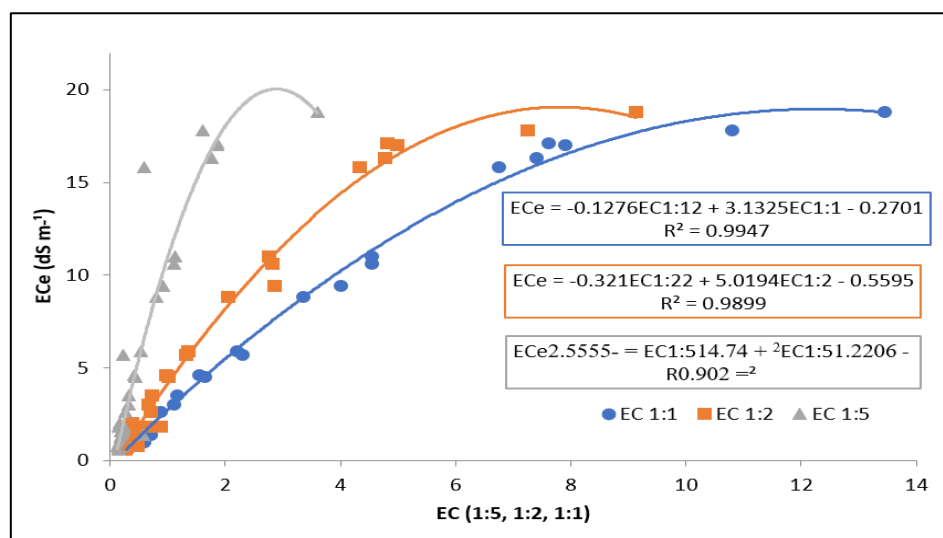


Figure 4: Quadratic model E_{Ce} vs. (EC 1:1, 1:2, 1:5)

The quadratic regression model in this study showed a significant improvement compared to the linear model, reflecting a well-known physical behavior for high ionic strength solutions. As ionic strength

increases, activity coefficients decrease according to the modified Debye–Hückel behavior, leading to a deviation between nominal concentration and actual conductivity [18]. Therefore, the assumption of linearity becomes inadequate at high salinity levels.

Cook's Distance Analysis

To evaluate the impact of influential points on the statistical models, Cook's Distance analysis was used to identify samples that might disproportionately affect the model results. The results showed (Table 5) that some samples in Kambout 2 and Haflez had high Cook's Distance values, indicating they might be influential points. These samples were classified as TRUE in the Cook's Distance table, while most other samples were under the accepted value (Cook's Distance < 1). The samples with high Cook's Distance may not represent the general environment of the depressions adequately, and therefore could be excluded. However, we decided to retain them in the analysis based on our finding that their impact on model accuracy was minimal and did not significantly affect the R² and RMSE values.

Table 5: Cook's Distance Test Results

Ec _x	Depression	Sample	EC _e	Ec _x	CooksD	Flag
EC1:1	Kampot2	C1	18.8	13.46	6.222652	TRUE
EC1:2				9.13	6.414679	
E1:5				3.6	10.34799	

Differences in Conversion Coefficients Between Depressions

ANCOVA was used to test the interaction between the depression and dilution extracts in this study. The purpose of this test was to examine whether the relationship between EC_e and dilution extracts (1:1 and 1:2) varies across depressions. ANCOVA analysis revealed (Table 6) a significant interaction between depression and dilution extracts (EC(1:1, 1:2), $p = 0.028, 0.044$), indicating that conversion coefficients are not constant across depressions. This demonstrates the need for local conversion equations rather than applying a general equation. In K2, where the average EC_e is more than four times higher than in the other depressions, the curvature was more pronounced. This supports the concept of local calibration rather than applying a general equation [17].

Table 6. ANCOVA Test Results

	sum_sq	df	F	PR(>F)
C(Depression)	5.633629	2	1.504566	0.234724
EC_1_1	796.7469	1	425.5723	1.38E-22
C(Depression):EC_1_1	14.65604	2	3.914171	0.028238
Residual	73.01492	39	--	--
C(Depression)	12.08432	2	2.394631	0.104494
EC_1_2	768.9304	1	304.7428	4.98E-20
C(Depression):EC_1_2	17.08219	2	3.385011	0.044099
Residual	98.40524	39	--	--
C(Depression)	51.80609	2	4.394778	0.019001
EC_1_5	633.8623	1	107.5427	9.05E-13
C(Depression):EC_1_5	20.68761	2	1.754957	0.186295
Residual	229.868	39	--	--

Performance Analysis Across Salinity Categories

(Figure 5) shows that the performance of the models clearly differs across salinity categories. The difference between the models was limited in the lower salinity categories (0–2 dS m⁻¹), indicating that the linear assumption is sufficient for the weak salinity range. As salinity increased, especially in the >10 dS m⁻¹ category, the linear model's error increased significantly, while the quadratic model maintained much lower RMSE values, reflecting its more suitable nature for representing non-linear behavior at high ionic strengths. The 1:5 extract showed relatively weaker performance in higher categories due to the significant dilution effect, which reduces sensitivity to great changes in salt concentration. These results suggest that the mathematical structure of the model should reflect the salinity system characteristics, especially in environments with a wide salinity gradient. Therefore, the choice of the optimal model should be based on the practical application range rather than solely on overall fit indicators (e.g., total R² values).

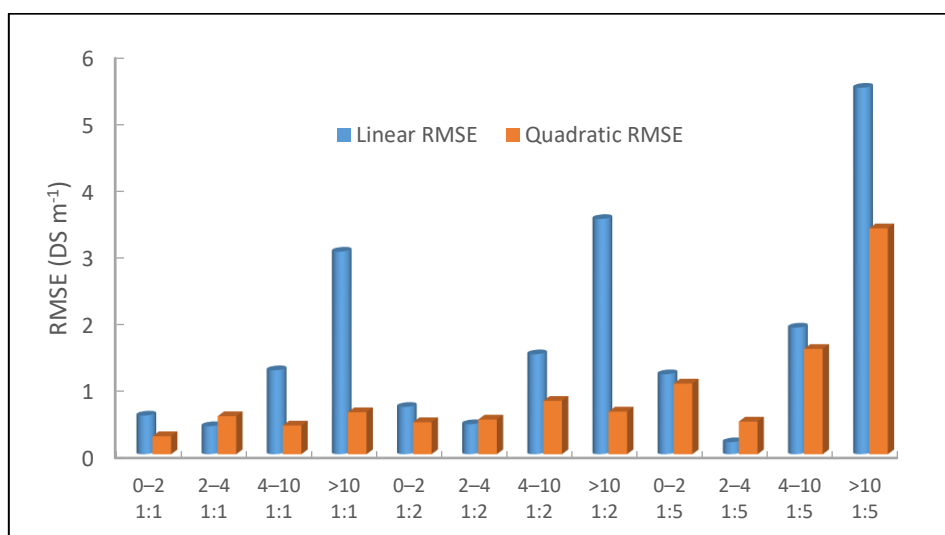


Figure 5. Performance of linear and quadratic models across salinity classes (RMSE comparison).

Conclusion

This study shows that the conversion relationships between water dilution extracts and the electrical conductivity of the saturated paste extract (EC_e) are not constant even within a limited geographic range, but are directly influenced by the intensity of the salinity system and the ionic variation range within the semi-arid depressions. The results indicated that the 1:1 and 1:2 extracts provide a high-accuracy representation of EC_e, with high predictive stability according to cross-validation. However, for characterizing environments with high salinity, non-linear models that reflect deviations from ideal solution behavior at high ionic strengths are required.

The noticeable improvement in performance when using the quadratic model, especially in the Northern Kambout depression, not only reflects statistical superiority but also represents a real change in conductivity response to increased salt concentration, consistent with ionic activity behavior in concentrated solutions. Additionally, the significance of the interaction test (ANCOVA) confirms that conversion coefficients differ based on the local geomorphological and salinity characteristics, highlighting the importance of regional calibration in salinity modeling studies.

At the applied level, the results suggest that using the 1:1 extract can provide a reliable operational alternative for estimating EC_e in semi-arid environments, maintaining a suitable balance between accuracy and analytical simplicity. In contrast, the quadratic model is more suitable when salinity spans a wide range or exceeds critical crop limits. Therefore, the developed equations offer a practical framework that can be integrated into field survey programs and rapid salinity assessment in internal drainage lowland systems. Despite the strong predictive performance, the sample size (n=45) remains moderate, and seasonal relationships may be influenced by variations in humidity and evaporation. Hence, the study recommends conducting multi-seasonal temporal calibration and testing the model in similar saline systems to assess regional transferability.

Acknowledgments

I would like to express my sincere thanks and appreciation to the administration of Tobruk University for their continuous support, as well as to the Faculty of Natural Resources and Environmental Sciences for overcoming obstacles, which contributed to the completion of this research.

Conflicts of Interest

There is no conflict of interest.

Note: Artificial Intelligence (ChatGPT 5.2) was used for proofreading and correcting spelling errors in this paper.

References

1. Richards LA, editor. Diagnosis and improvement of saline and alkali soils. Washington (DC): U.S. Government Printing Office; 1954. (USDA Handbook No. 60).
2. Corwin DL, Yemoto K. Salinity: electrical conductivity and total dissolved solids. In: Bigham JM, editor. Methods of soil analysis: chemical methods. Madison (WI): Soil Science Society of America; 2020.
3. Ouzemou JE, Laamrani A, El Battay A, et al. Predicting soil salinity based on soil/water extracts in a semi-arid region of Morocco. *Soil Syst.* 2025;9(1):3. doi: 10.3390/soilsystems9010003.

4. Khorsandi F, Yazdi FA. Estimation of saturated paste extracts' electrical conductivity from 1:5 soil/water suspension and gypsum. *Commun Soil Sci Plant Anal.* 2011;42(3):311–321. doi: 10.1080/00103624.2011.538885.
5. Smagin A, Kacimov A, Sadovnikova N. EC conversion for 1:5 extracts and standard saturated soil-water pastes in the assessment of arid land salinization: classical methodologies revisited. *J Saudi Soc Agric Sci.* 2023. doi: 10.1016/j.jssas.2023.12.005.
6. He Y, DeSutter T, Hopkins D, Jia X, Wysocki DA. Predicting ECe of the saturated paste extract from value of EC1:5. *Can J Soil Sci.* 2013;93(5):585–594. doi: 10.4141/cjss2012-080.
7. James G, Witten D, Hastie T, Tibshirani R. *An introduction to statistical learning: with applications in R.* 2nd ed. New York (NY): Springer; 2021. doi: 10.1007/978-1-0716-1418-1.
8. Chai T, Draxler RR. Root mean square error (RMSE) or mean absolute error (MAE)? Arguments against avoiding RMSE in the literature. *Geosci Model Dev.* 2014;7:1247–1250. doi: 10.5194/gmd-7-1247-2014.
9. Soliman MMM. The effect of the North Atlantic Oscillation (NAO) on rainfall in the Tobruk region (1985–2018). *J Fac Arts Univ Benghazi.* 2021;(5):88–109. doi: 10.37376/jfofa.vi50.4455.
10. Abas MFA, Abdulqadir HFY, Ajweedah FIM. Validity of groundwater for use in irrigation and estimation of soil salinity for Hafalaz region (east of Tobruk city, Libya). *Al-Salam Int Univ J.* 2022;12:98–110.
11. Li X, McCarty G. Application of topographic analyses for mapping spatial patterns of soil properties. *Earth Obs Geospat Anal.* 2019. doi: 10.5772/intechopen.86109.
12. Callow J, Hipsey M, Vogwill R. Surface water as a cause of land degradation from dryland salinity. *Hydrol Earth Syst Sci.* 2020;24:717–733. doi: 10.5194/hess-24-717-2020.
13. Yu F, Harbor J. The effects of topographic depressions on multiscale overland flow connectivity: a high-resolution spatiotemporal pattern analysis approach based on connectivity statistics. *Hydrol Process.* 2019;33:1403–1419. doi: 10.1002/hyp.13409.
14. Chaves HML, Montalvão MTL, Fonseca MRS. Mapping wet areas and drainage networks of data-scarce catchments using topographic attributes. *Water.* 2025;17(15). doi: 10.3390/w17152298.
15. Loritz R, Kleidon A, Jackisch C, Westhoff M, Ehret U, Gupta H, Zehe E. A topographic index explaining hydrological similarity by accounting for the joint controls of runoff formation. *Hydrol Earth Syst Sci.* 2019;23:3807–3824. doi: 10.5194/hess-23-3807-2019.
16. Al-Zoubi MM, Al-Hasani AM, Dargam H. *Methods of soil, water, plant, and fertilizer analysis.* Syria: Ministry of Agriculture and Agrarian Reform; 2013.
17. Slavich P, Petterson G. Estimating the electrical conductivity of saturated paste extracts from 1:5 soil, water suspensions and texture. *Aust J Soil Res.* 1993;31:73–81. doi: 10.1071/SR9930073.
18. Stumm W, Morgan JJ. *Aquatic chemistry: chemical equilibria and rates in natural waters.* 3rd ed. New York (NY): Wiley; 1996.

Appendix 1. Sample Analysis Results and Geographic Coordinates

Depression	Sample	ECe	EC1:1	EC1:2	EC1:5	pH	Texture	N	E
Hafilz	W1	1.8	0.35	0.88	0.14	7.9	sandy loam	31.827256°	24.465879°
Hafilz	W2	1.4	0.47	0.3	0.57	7.99	sandy loam	31.829477°	24.466460°
Hafilz	W3	1.3	0.57	0.47	0.19	7.7	loam	31.831142°	24.466895°
Hafilz	W4	1	0.59	0.39	0.22	7.94	loam	31.832807°	24.467331°
Hafilz	W5	0.8	0.41	0.47	0.2	8.02	loam	31.835028°	24.467912°
Hafilz	C1	9.4	4.01	2.86	0.91	7.51	sandy loam	31.822495°	24.484721°
Hafilz	C2	0.8	0.34	0.27	0.14	8.06	sandy loam	31.825002°	24.485377°
Hafilz	C3	1.5	0.68	0.45	0.24	7.8	loam	31.826882°	24.485869°
Hafilz	C4	1.1	0.5	0.36	0.22	7.93	sandy loam	31.828762°	24.486361°
Hafilz	C5	3	1.1	0.66	0.32	7.81	loam	31.831269°	24.487017°
Hafilz	E1	2.6	0.88	0.71	0.26	7.88	sandy loam	31.819931°	24.504136°
Hafilz	E2	1.3	0.53	0.36	0.18	8.04	sandy loam	31.821421°	24.504527°
Hafilz	E3	0.8	0.31	0.25	0.13	8.19	sandy loam	31.822538°	24.504819°
Hafilz	E4	4.6	1.55	0.97	0.41	7.87	sandy loam	31.823655°	24.505112°
Hafilz	E5	1.2	0.45	0.31	0.18	8.08	sandy loam	31.825145°	24.505502°
Kampot1	W1	0.92	0.34	0.25	0.14	8.15	sandy loam	31.886411°	24.432108°
Kampot1	W2	0.9	0.41	0.28	0.17	8.18	sandy loam	31.887718°	24.432079°
Kampot1	W3	1	0.51	0.3	0.22	8.16	sandy loam	31.888698°	24.432057°
Kampot1	W4	1.3	0.51	0.31	0.22	8.03	loam	31.889678°	24.432035°
Kampot1	W5	10.6	4.55	2.82	1.1	7.62	loam	31.890985°	24.432006°
Kampot1	C1	3.5	1.16	0.73	0.33	7.87	sandy loam	31.885915°	24.451380°
Kampot1	C2	1.7	0.64	0.43	0.22	8.12	sandy loam	31.886929°	24.451358°
Kampot1	C3	0.7	0.28	0.26	0.14	7.95	sandy loam	31.887689°	24.451341°

Kampot1	C4	0.9	0.36	0.29	0.15	7.7	sandy loam	31.888450°	24.451324°
Kampot1	C5	0.6	0.3	0.26	0.14	8.06	sandy loam	31.889464°	24.451302°
Kampot1	E1	1.8	0.7	0.7	0.24	7.82	sandy loam	31.887787°	24.470601°
Kampot1	E2	0.8	0.35	0.23	0.15	7.9	sandy loam	31.889671°	24.470560°
Kampot1	E3	0.8	0.36	0.27	0.14	8.13	sandy loam	31.891084°	24.470529°
Kampot1	E4	0.95	0.47	0.31	0.18	8.02	silt loam	31.892496°	24.470498°
Kampot1	E5	4.5	1.65	1.02	0.44	8.01	sandy loam	31.894380°	24.470457°
Kampot2	W1	11	4.54	2.75	1.12	7.54	loam	31.934932°	24.457421°
Kampot2	W2	5.7	2.3	1.32	0.22	7.69	loam	31.936603°	24.457608°
Kampot2	W3	17.8	10.81	7.26	1.6	7.94	loam	31.937857°	24.457748°
Kampot2	W4	2	0.39	0.37	0.16	8.12	loam	31.939111°	24.457889°
Kampot2	W5	15.8	6.76	4.33	0.59	7.51	sandy loam	31.940783°	24.458076°
Kampot2	C1	18.8	13.46	9.13	3.6	7.41	loam	31.931134°	24.471302°
Kampot2	C2	17	7.91	4.98	1.86	7.65	sandy loam	31.933592°	24.471578°
Kampot2	C3	16.3	7.4	4.77	1.77	7.54	sandy loam	31.935436°	24.471784°
Kampot2	C4	1.6	0.55	0.38	0.19	8.05	loam	31.937280°	24.471991°
Kampot2	C5	0.85	0.42	0.34	0.18	7.47	sandy loam	31.939738°	24.472267°
Kampot2	E1	17.1	7.62	4.82	1.86	7.62	sandy loam	31.932121°	24.485719°
Kampot2	E2	8.8	3.36	2.04	0.8	7.71	loam	31.934348°	24.485970°
Kampot2	E3	5.9	2.2	1.35	0.54	7.78	loam	31.936018°	24.486157°
Kampot2	E4	1.4	0.7	0.42	0.22	7.97	silt loam	31.937688°	24.486345°
Kampot2	E5	0.9	0.38	0.3	0.16	8	sandy loam	31.939915°	24.486595°